

An Algorithm for Computing Side Lobe Values of a Designed NLFM function

N. Adithyavalli¹, D. Elizabeth Rani², C. Kavitha³^{1,2}Department of Electronics and communication Engineering Gitam University, Visakhapatnam, India,¹adithyavalli@gmail.com, ²elizabeth.varghese@gitam.edu³Department of Physics, Gitam University, Visakhapatnam, India

kavitha.chandu@gitam.edu



ABSTRACT

Several applications in radar systems entail low range side lobe performance to identify the targets. It is achieved by pulse compression processing. The chirp signal also known as linear frequency modulation (LFM) signal is most widely used for this purpose. Since it exhibits high first side-lobe value in the autocorrelation, non linear chirp signals (NLFM) are introduced as a solution to suppress the sidelobes. NLFM signals can be generated by using simple two-stage piece wise linear frequency modulation (PWLFM) functions. The chirp rates of the two stages are selected differently. This NLFM signal exhibited better peak to sidelobe level (PSLR) values compared to its counterpart LFM signal. In this paper we present a complete contour map of the computed side lobe values, to identify the optimum chirp rates of the two stages. The side lobes are computed based on algorithm written in python scripting language. This map helped us to identify two interwoven fluctuations in the spectrum of side-lobe values that can be used to decide the breakpoint value for a given bandwidth and pulse width. The best NLFM is generated by identifying the optimum slopes of the two LFM stages, which is further combined with the windows functions to achieve a significant reduction in PSLR.

Key words: Contour, LFM, NLFM, PSLR, PWLFM.

1. INTRODUCTION

Radar systems employ pulse compression as it can resolve the contradiction between range resolution and average transmitted power effectively [1]. The key attributes of pulse compression system should be a large time-bandwidth product (high compression ratio) for better range resolution, low time side-lobe and less sensitivity level of side-lobe level to Doppler shift [2]. Various modulation schemes are available, such as Linear Frequency Modulation (LFM), Non-Linear Frequency Modulation (NLFM) and Time-frequency coded waveforms (Costas Codes). Since World War II, LFM or chirp waveform is the most accepted

pulse compression method as they have superior performance, which can be easily generated and processed. The frequency is increased or decreased over the pulse duration either upward (up-chirp) or downward (down-chirp). The instantaneous frequency of up-chirp LFM is given by

$$f(t) = f_0 + \mu t \quad (1)$$

Where, f_0 is the radar center frequency, and $\mu = (2\pi B)/\tau$ is the LFM coefficient, B =bandwidth and τ is pulse width. Similarly, the instantaneous frequency for down-chirp LFM is given by

$$f(t) = f_0 - \mu t \quad (2)$$

Adding linear frequency modulation widens the bandwidth and because of this, the range resolution enhances by a factor equal to the time-bandwidth product [3]. Yet, the LFM has large side-lobes in matched filter output which is the major drawback for which amplitude weighting (windowing) or data tapering is required to reduce the side lobes. It certainly drops the SNR value typically by 1-2 dB [4]. High side-lobes are unacceptable as they may mask the presence of weaker targets echo signals. When the side-lobe levels are comparatively low, nearby weaker targets echo can be easily renowned from the stronger targets echo [5]. Linear FM has uniform spectrum as transmitter gives equal time to each frequency, modification to this uniform spectrum by deviating the rate of change of frequencies is termed as Non-linear frequency modulation (NLFM) [6]. NLFM is favoured as it can shape the power spectral density (PSD) such that the autocorrelation function showcases profoundly reduced side-lobes from its analogues LFM. Consequently, no additional filtering is required and maximum SNR performance is preserved [7]. Several research works has been done to design better NLFM signals, all the work done generally can be categorized into two directions [8-10]. One is based on design by using predefined power spectral density function using different methods as iterative methods, stationary phase principle and explicit functions cluster method and the other method is to design NLFM signal using LFM signals introducing predistortion on short intervals into spectral domain or temporal domain [11].

In the present work, a non linear waveform from optimized piecewise linear functions was proposed and shown to be experimentally effective with respect to a LFM chirp signal. It is proposed to design a NLFM signal using two stage LFM functions. The optimum value of the slopes of the two LFM functions are found by identifying the breakpoints in the contour map of the PSLR values obtained for the various possible slopes. For the best NLFM signal designed, window functions are applied for further reduction of side lobes.

2. THE TWO-STAGE NLFM

A NLFM signal is generated using simple two-stage PWLFM functions as shown in Figure 1. It has two LFM stages with distinct sweep rates.

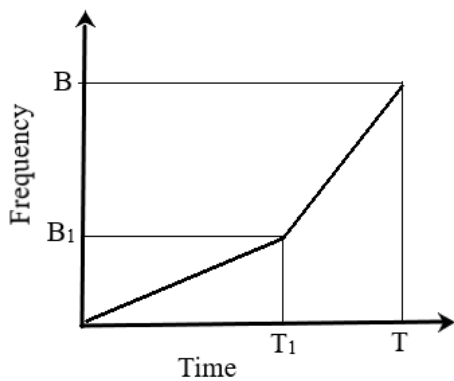


Figure 1: Two stage PWLFM function

$$f(t) = \begin{cases} \alpha_0 t & 0 \leq t \leq T_1 \\ B_1 + \alpha_1(t - T_1) & T_1 \leq t \leq (T_1 + T_2) \end{cases} \quad (3)$$

Equation (3) represents the variation of instantaneous frequency of NLFM signal formed by concatenating two piece wise LFM functions with a sweep rate of α_0 and α_1 in the respective first and second stages. The total pulse width of the chirp signal τ is divided into two time slots with respective pulse widths T_1 and T_2 . If B_1 and B_2 are the corresponding bandwidths of the first and second stage LFM functions, then the corresponding sweep rates can be defined as

$$\alpha_0 = \frac{B_1}{T_1} \quad \alpha_1 = \frac{B_2}{T_2}$$

The corresponding phase variation of this concatenated NLFM function can be obtained by integrating (3)

$$\varphi(t) = \int f(t) dt = \begin{cases} \alpha_0 \frac{t^2}{2} & 0 \leq t \leq T_1 \\ B_1 t + \alpha_1 (\frac{t^2}{2} - T_1 t) & T_1 \leq t \leq T_1 + T_2 \end{cases} \quad (4)$$

Simulations are done with $B = 20$ MHz and $T = 10 \mu s$ with different combinations of B_1 , T_1 and B_2 , T_2 . All the possible combinations are examined by choosing different sweep rates α_0 , α_1 for both PWLFM functions. Break point B_1 is kept

constant at 6MHz and simulations were done for different T_1 values, the corresponding PSLR values are tabulated in the following Table 1.

Table 1: PSLR values of two stages PWLFM function with different T_1 values.

B_1 (MHz)	T_1 (μs)	PSLR(dB)
6	2	-9.31
	4	-15.57
	5	-21.99
	6	-20.55
	8	-17.86
	9	-16.24

Figure 2(a)-5(a) shows the frequency variation of PWLFM function when B_1 is kept constant and T_1 is varying from $2 \mu s$ to $9 \mu s$, and the corresponding matched filter outputs are shown in Figure 2(b)-5(b). From the above Table 1 and below figures it is observed that the PSLR values are increasing when the break point (T_1) value is increasing in the leading edge region and reached maximum value of -21.99dB exactly at $T_1=5 \mu s$, then from there again PSLR value is decreasing when the break point (T_1) value is approaching the trailing edge region.

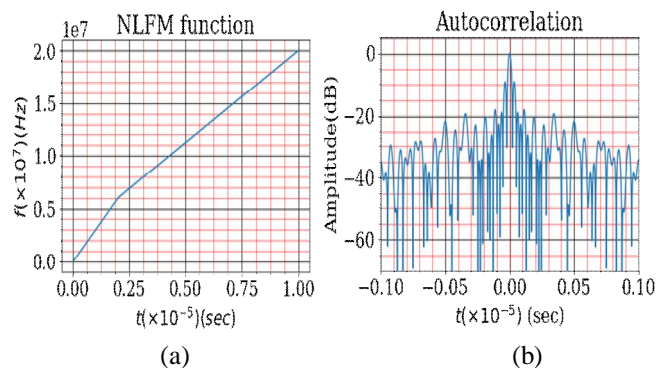


Figure 2: (a) PWLFM function with $B_1=6$ MHz, $T_1=2 \mu s$ (b) Matched filter output

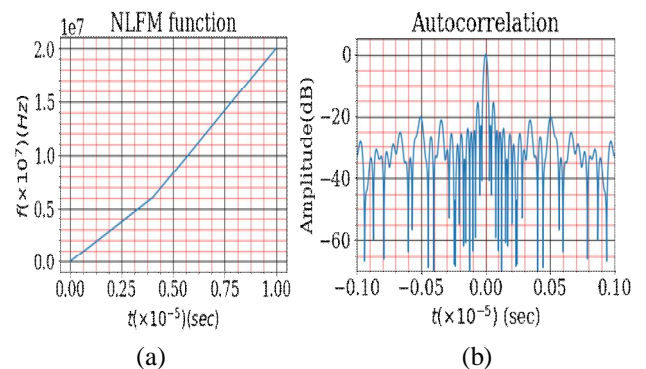


Figure 3: (a) PWLFM function with $B_1=6$ MHz, $T_1=4 \mu s$ (b) Matched filter output

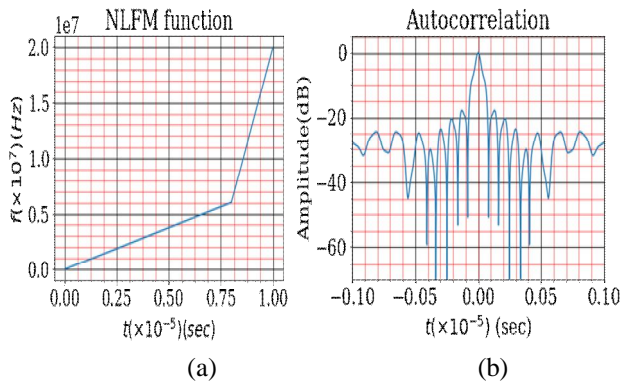


Figure 4: (a) PWLFM function with $B_1=6\text{MHz}$, $T_1=8\mu\text{s}$ (b) Matched filter output

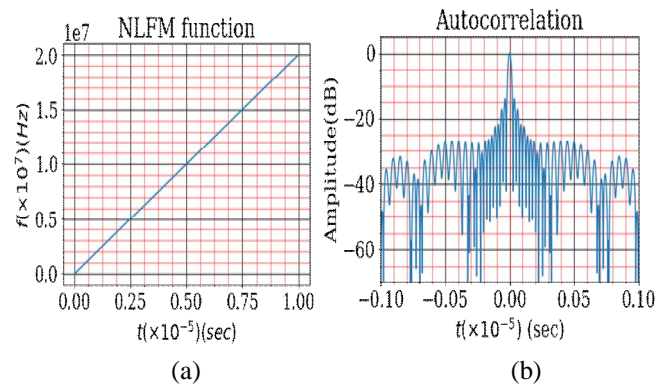


Figure 7: (a) PWLFM function with $\alpha_0=2$, $\alpha_1=2$ (b) Matched filter output

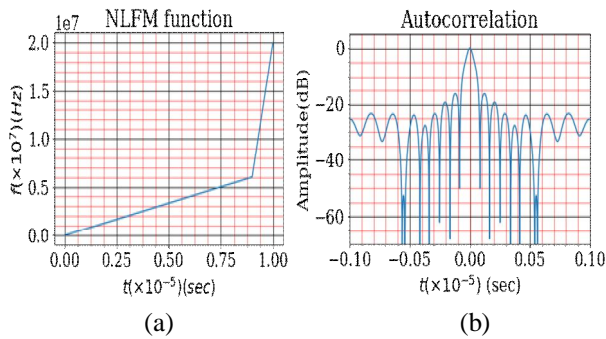


Figure 5: (a) PWLFM function with $B_1=6\text{MHz}$, $T_1=9\mu\text{s}$ (b) Matched filter output

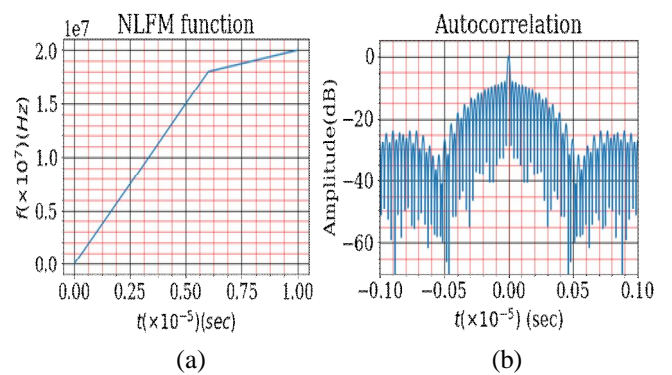


Figure 8: (a) PWLFM function with $\alpha_0=3$, $\alpha_1=0.5$ (b) Matched filter output

Figure 6(a) shows the frequency variation of two stage NLFM function with $B_1=6\text{MHz}$ and $T_1=5\mu\text{s}$ and achieved PSLR value of -21.99dB as shown in Figure 6(b). Figure 7(a) shows the frequency variation with $B_1=14\text{MHz}$ and $T_1=7\mu\text{s}$ which yielded a PSLR value of -14.04dB as shown in Figure 7(b). Figure 8(a) shows the frequency variation with $B_1=18\text{MHz}$ and $T_1=6\mu\text{s}$ and achieved PSLR value of -8.28dB as shown in Figure 8(b).

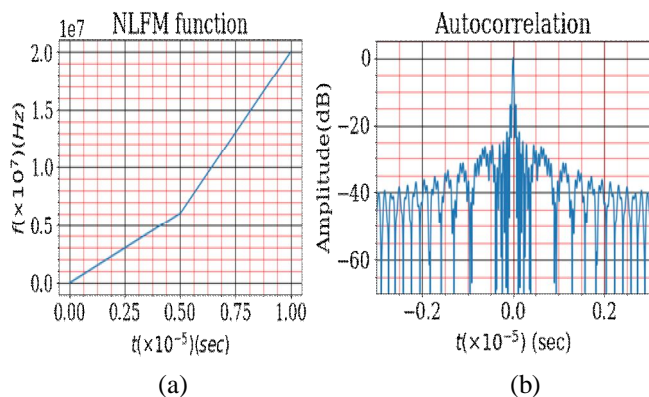


Figure 6: (a) PWLFM function with $\alpha_0=1.2$, $\alpha_1=2.8$ (b) Matched filter output

Similarly simulations were performed by changing the values of B_1 and T_1 simultaneously and an attempt is made to observe the PSLR variations based on various sweep rate ratios. Table 2 shows the variation of PSLR values depending upon the sweep rate ratio. It is observed that there is a significant increase in PSLR value when the sweep rate ratio α_0 of first stage LFM function has a lower value and sweep rate ratio α_1 of second stage LFM function has a higher value.

Table 2: Sweep Rate Ratios for Different Combinations of T_1 , B_1 , T_2 , B_2 and Corresponding PSLR values.

$\alpha_0=B_1/T_1$	$\alpha_1=B_2/T_2$	PSLR(dB)
1.2	2.8	-21.99
1.6	2.5	-20.70
1.7	2.4	-18.27
2	2	-14.04
2.25	1	-12.42
2.57	0.66	-10.42
3	0.5	-8.28

Simulations were carried for different bandwidth values, B=2MHz, 20MHz and 40MHz with T=10μs. Table 3 shows the PSLR values for different values of time-bandwidth (BT) products. It is observed that the PSLR value is reducing with increasing BT product. When BT product is 20 PSLR value of -18.30dB is achieved when sweep rate ratio are α₀=0.04 and α₁=1.6, When BT is 200 the PSLR value of -21.99dB for α₀=1.2 and α₁=2.8 and when BT is 400 the PSLR value of -23.02dB is achieved with sweep rates of α₀=2 and α₁=5.3.

Table 3: PSLR values for different Time-Bandwidth (BT) products.

B(MHz)	T(μs)	BT	α ₀ =B ₁ /T ₁	α ₁ =B ₂ /T ₂	PSLR(dB)
2	10	20	0.04	1.6	-18.30
20	10	200	1.2	2.8	-21.99
40	10	400	2	5.3	-23.02

3. ALGORITHM AND CONTOUR PLOT

Instead of analyzing all the numerical values of PSLR value for each value of B₁ and T₁, we made use of the contour plot to study the side lobe variations at all possible values of the break-points (B₁, T₁) of NLFM where B and T are the bandwidth and pulse duration of the signal. The function (see Figure 1) is chosen with break-points at (B₁, T₁). The autocorrelation of the real part of chirp signal s(t) defined as in (5)

$$s(t) = \exp\{j2\pi(f_c t - 1/2kt^2)\} \tag{5}$$

is used to find the sidelobe values where f_c is the carrier frequency and k is the chirp rate or sweep rate of the waveform respectively. The sidelobe values have been calculated for nearly the entire range of breakpoints (B₁, T₁). The following algorithm is used for calculating the PSLR values and the contour map is plotted using python script. Where s(t) is the chirp signal, Xcorr is the autocorrelation of s(t), SL(Xcorr) is the first sidelobe value for Xcorr. The autocorrelation function is computed for the chirp signal and then first sidelobe value is obtained by identifying the first zero from the right hand side of the autocorrelation plot and the peak value next to zero is identified as first sidelobe value and the entire procedure is repeated for the complete range of B₁ and T₁.

Algorithm 1 Computing the contour map of a two-stage NLFM function.

Procedure NLFM 2-STAGE CONTOUR

```

for B1 in B1 range do
  for T1 in T1 range do
    Xcorr (B1, T1) ← autocorr[s (t, B1, T1)]
    PSLR (B1, T1) ← SL (Xcorr (B1, T1))
  
```

```

end for
end for
The data for PSLR (B1, T1) is stored in a file or plotted as a
contour for visual reference.
end procedure
Procedure SL (Xcorr (B1, T1))
Find the first zero in the right half of Xcorr (B1, T1).
SLloc ← B1 location of the subsequent maxima
(M1).
SLval ← Peak value of M1.
Return SLloc and SLval
end procedure

```

PSLR is calculated with B=20MHz and T=10μs for 0.1 resolution and 0.001 resolution and it is plotted in the three dimensional plot as a function of normalized values of B₁ and T₁ (B₁/B and T₁/T). To yield more accurate position of side lobe value two different resolutions were chosen. For 0.1 resolution, the PSLR value attained is -21.99dB and for 0.001 resolution the PSLR value attained is -26.26dB. As the side lobe values are very sensitive to the break point locations accurate values of PSLR were found with finest resolution. Figure 9(a) and 10(a) shows the contour maps of two stage NLFM function with 0.1 and 0.001 resolutions. It is amply clear that high sidelobe values are confined to the region above the main diagonal of the (B₁, T₁) grid.

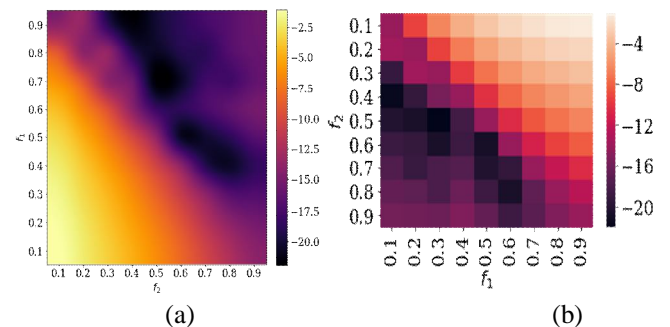


Figure 9: (a) Contour map of sidelobe values as a function of the break-points, f₁ = B₁/B and f₂ = T₁/T, where B=20MHz and T=10μs with 0.1 resolution (b) Heat Map

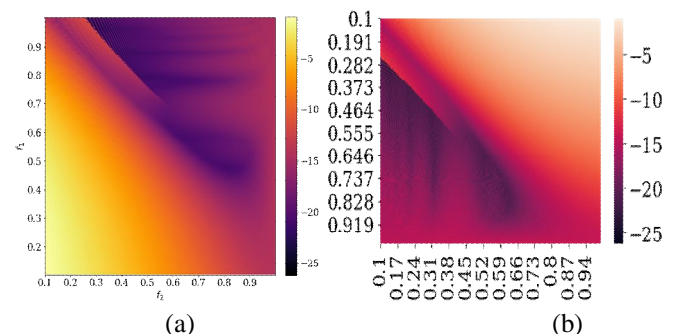


Figure 10: (a) Contour map of sidelobe values as a function of the break-points, f₁ = B₁/B and f₂ = T₁/T, where B=20MHz and T=10μs with 0.001 resolution (b) Heat Map

Figure 9(b) and 10(b) shows the heat maps of PSLR values. From the heat map the lowest PSLR value obtained can be clearly identified based on the value represented by different colors on color bar and the corresponding break points B_1 , T_1 can be calculated using $B_1=f_1*B$ and $T_1=f_2*T$. Further from the heat maps a mask can be made to the f_1 and f_2 region where the highest PSLR values are obtained. Figure 11(a) shows the mask made from the heat map (see Figure 9(b)) for PSLR values above -20dB. From the color bar right to the heat map, the darkest black color indicate the highest PSLR (-21.99dB) value (see Table 1) which is obtained for $f_1=0.3$ and $f_2=0.5$ and the corresponding B_1 ($B_1=f_1*B$ (20MHz)) =6MHz, T_1 ($T_1=f_2*T$ (10 μ s)) =5 μ s values. Similarly from the below Figure all other regions for entire PSLR values can be identified. Similarly Figure 11(b) shows the mask made from the heat map (see Figure 10(b)) for PSLR values above -25dB. From the color bar right to the heat map, the darkest black color indicate the highest PSLR (-26.26dB) value which is obtained for $f_1=0.112$ and $f_2=0.271$ and the corresponding B_1 ($B_1=f_1*B$ (20MHz)) =2.24MHz, T_1 ($T_1=f_2*T$ (10 μ s)) =2.71 μ s values.

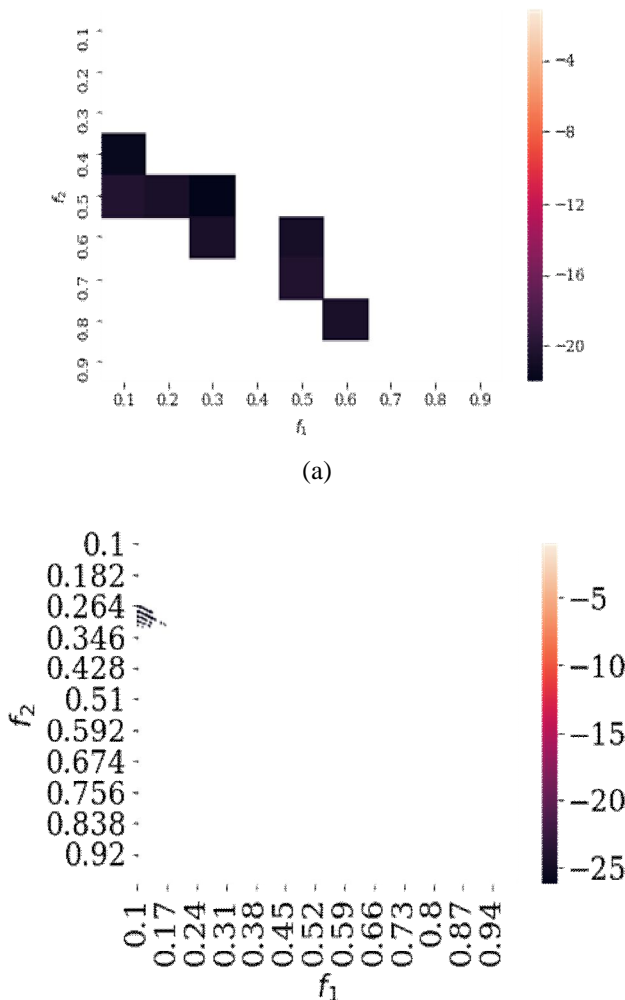


Figure 11: (a) Mask of heat map (see Figure 9(b)) for above -20dB PSLR values (b) Mask of heat map (see Figure 10(b)) for above -25dB PSLR values

4. WINDOW WEIGHTING

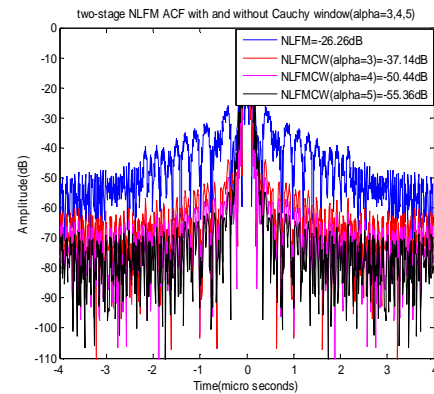
The whole set of PSLR values of the two stages NLFM function designed is explored using contour analysis for the entire region of break points B_1 and T_1 . To further reduce the PSLR values window function is applied to the two stage NLFM function. PSLR value of -26.26dB is attained at $B_1=2.24$ MHz and $T_1=2.71\mu$ s for the designed NLFM function. To further reduce the PSLR value two flexible window functions named Cauchy and power of cosine are applied. The window functions used are described below. The matched filter (MF) output characteristics depend upon the variable parameters alpha (α) and P.

1) Cauchy window

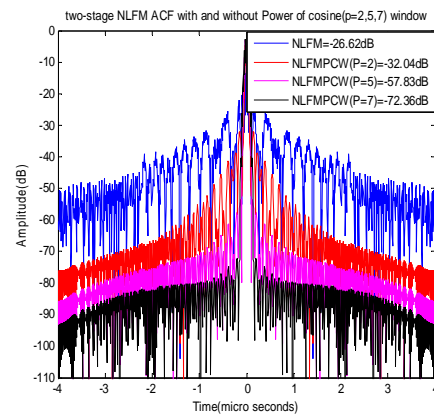
$$w(n) = \frac{1}{1 + (\alpha \frac{n}{N/2})^2} \quad 0 \leq |n| \leq N/2$$

2) Power of Cosine window

$$w = \cos^p \left(\frac{\pi n}{N} \right) \quad n = -\frac{(N-1)}{2}; \frac{(N-1)}{2}$$



(a)



(b)

Figure 12: Matched filter output (a) Cauchy (b) Power of cosine

5. CONCLUSION

We have presented a nearly complete map of the side lobe values for a two-stage NLFM signal. The main purpose of the contour plot is to identify the portion of break point B1 and T1 which yields the lowest PSLR values. Simulations were made for different resolutions to obtain more accurate PSLR values. The lowest PSLR value for the designed two stage NLFM function is -26.26dB for 0.001 resolutions and -21.99dB for 0.1 resolutions. To further reduce the PSLR values two window functions were applied. There is a considerable drop in the values of PSLR from -26.26dB to -55.36 dB and to -72.36dB respectively when Cauchy ($\alpha=5$) and Power of cosine ($p=7$) window functions were applied. The designed signal here is an NLFM which can be easily generated by using two piecewise linear, continuous segments. This method reveals two interwoven fluctuations in the spectrum of side-lobe values that can be used to decide the breakpoint value for a given bandwidth and pulse width. This technique may be extended to other multistage signals consisting of piecewise linear segments and Optimization.

REFERENCES

1. F. U. Yin-juan and P. Rou-yo, 2012 “**Research on Pulse Compression Technology of Linear Frequency Modulation Signal**”, in International Conference on Industrial control and Electronics Engineering, China. <https://doi.org/10.1109/ICICEE.2012.300>
2. A. W. Doerry, 2006 “**Generating Nonlinear FM Chirp Waveforms for Radar**”, Technical Report, Sandia National Laboratories, September. <https://doi.org/10.2172/894743>
3. N. Touati, C. Tatkeu, T. Chonavel and A. Rivenq, 2013 “**Doubly coded Costas signals for grating lobes mitigation**,” 2013 IEEE 24th Annual International Symposium on Personal, Indoor, and Mobile Radio Communications (PIMRC), London, pp. 481-485. <https://doi.org/10.1109/PIMRC.2013.6666184>
4. S. Golomb and H. Taylor, 1984 “**Constructions and Properties of Costas arrays**”, Proceedings of the IEEE, vol. 72, no. 9, pp. 1143-1163. <https://doi.org/10.1109/PROC.1984.12994>
5. Y. K. Chan, M. Y. Chua and V. C. Koo, 2009 “**Sidelobe reduction using simple two and tri-stages non-linear frequency modulation**”, in Journal of progress In Electromagnetic Research, vol.98, pp.33-52. <https://doi.org/10.2528/PIER09073004>
6. I. C. Vizitiu, F. Enache and F. Popescu, 2014 “**Sidelobe Reduction in Pulse-Compression Radar Using the Stationary Phase Technique: an Extended Comparative Study**”, in International Conference on Optimization of Electrical and Electronic Equipment. <https://doi.org/10.1109/OPTIM.2014.6850932>
7. L. Anton, 2008 **Signal Processing** in HR radars, MTA.
8. S. Boukeffa, Y. Jiang and T. Jiang, 2011 “**Sidelobe reduction with nonlinear frequency modulation waveforms**”, in Proc. of the IEEE CSPA conference, pp. 399-403. <https://doi.org/10.1109/CSPA.2011.5759910>
9. Maria Zemzami, Aicha Koulou, Norelislam Elhami, Mhamed Itmi and Nabil Hmina, “**Interoperability Optimization using a modified PSO algorithm**”, International Journal of Advanced Trends in Computer Science and Engineering, Vol.8, No.2, pp-101- 107, 2019. <https://doi.org/10.30534/ijatcse/2019/01822019>
10. Anita Kulkarni and Dr. Elizabeth Rani, “**Unconstraint 2-Level Cost Optimization Coding for Signal Processing**”, International Journal of Advanced Trends in Computer Science and Engineering, Vol.8, No.1, pp-93- 100, 2019. <https://doi.org/10.30534/ijatcse/2019/15812019>
11. I. Vizitiu, L. Anton, F. Popescu and G. Iubu, 2012 “**The synthesis of some NLFM laws using the stationary phase principle**,” 2012 10th International Symposium on Electronics and Telecommunications, Timisoara, pp. 377-380. <https://doi.org/10.1109/ISETC.2012.6408053>